AIAA JOURNAL
Vol. 30, No. 2, February 1992

Convergence Improvement for Component Mode Synthesis

Remi C. Engels*
University of Tennessee Space Institute, Tullahoma, Tennessee 37388

Model order reduction by component mode synthesis relies on the truncation of high-frequency component modes. Such truncations inevitably lead to approximate solutions for the system frequencies and mode shapes. A technique is proposed to improve the accuracy of the computed system modal content. An upper bound is derived for the norm of the residual vector corresponding to each eigenvalue-eigenvector pair. The proposed scheme is aimed at lowering this upper bound, thereby consistently improving the overall accuracy of the system eigen solution. This method is not designed to lead to complete convergence. However, significant improvement is consistently obtained at virtually no cost and by using only practically available information. Numerical examples are included for demonstration purposes.

Introduction

COMPLEX structural systems are often divided into smaller, more manageable components or substructures. During the early design stages, much of the analysis is accomplished at the component level, usually by different organizations. This early organizational independence has, of course, obvious advantages. However, at some point in time, a system model is needed in order to study component interactions.

Component mode synthesis techniques were specifically developed to assemble already existing component models. References 1–5 represent a selection of the original work on substructuring techniques, and Refs. 6–8 contain detailed surveys. Following the assumed modes method, the system displacement vector is directly written as a linear combination of component assumed modes. In addition, interface compatibility between the various components is enforced. The final equations of motion for an undamped structural system undergoing free vibrations take on the form

$$M\ddot{u} + Ku = 0 \tag{1}$$

where the system displacement vector u, the mass matrix M, and the stiffness K matrix are given by

$$u = \begin{Bmatrix} u_I \\ q \end{Bmatrix} \tag{2}$$

$$M = \begin{bmatrix} M_{II} & M_{IN} \\ M_{IN}^T & I \end{bmatrix} \tag{3}$$

$$K = \begin{bmatrix} K_{II} & 0 \\ 0 & \Lambda \end{bmatrix} \tag{4}$$

The vectors u_I and q represent the interface and modal displacement vectors, respectively. The diagonal matrix Λ contains the frequencies Λ_i of all the component modes to be included in the model. The matrices M_{II}, M_{IN}, and K_{II} are known and depend on the type of component mode synthesis technique used. The IN partition in K vanishes automatically only when interface restrained assumed modes are employed.[9] However, it can be shown that this partition can be taken as zero, without loss of generality, even when other types of component modes are used.

An important feature of component mode synthesis techniques is that they allow for modal truncation in a natural manner. Indeed, high-frequency component modes generally contribute little to the low-frequency response of the complete system. Therefore, a cutoff frequency Λ_c is computed on the basis of the desired fidelity Λ_d of the complete system model

$$\Lambda_c = r^* \Lambda_d \tag{5}$$

where r^* is a factor between 2 and 9, taken from experience. It is then customary to truncate all component modes with frequency Λ_i larger than Λ_c. This is equivalent to constraining the corresponding modal coordinates in q.

The modal displacement vector q in Eq. (2) can then be partitioned as follows

$$q = \begin{Bmatrix} q_1 \\ q_2 \end{Bmatrix} \tag{6}$$

where q_2 contains all modal coordinates to be neglected. Correspondingly, Eq. (1) can be written as

$$\begin{bmatrix} M_{II} & M_{IN1} & M_{IN2} \\ M_{IN1}^T & I & 0 \\ M_{IN2}^T & 0 & I \end{bmatrix} \begin{Bmatrix} \ddot{u}_I \\ \ddot{q}_1 \\ \ddot{q}_2 \end{Bmatrix} + \begin{bmatrix} K_{II} & 0 & 0 \\ 0 & \Lambda_1 & 0 \\ 0 & 0 & \Lambda_2 \end{bmatrix} \begin{Bmatrix} u_I \\ q_1 \\ q_2 \end{Bmatrix} = \begin{Bmatrix} 0 \\ 0 \\ 0 \end{Bmatrix} \tag{7}$$

where the appropriate definitions are easily inferred from Eqs. (2–4) and (6). The diagonal matrix Λ_2 contains all component mode frequencies larger than Λ_c. The final reduced order model for the system is obtained from Eq. (7) by striking out the rows and columns corresponding to q_2. An eigenvalue problem can now be formulated as follows

$$\rho_i \begin{bmatrix} M_{II} & M_{IN1} \\ M_{IN1}^T & I \end{bmatrix} \phi_i = \begin{bmatrix} K_{II} & 0 \\ 0 & \Lambda_1 \end{bmatrix} \phi_i \tag{8}$$

where ρ_i and ϕ_i are a generic eigenvalue-eigenvector pair satisfying Eq. (8).

The eigenvalues ρ_i and vectors ϕ_i are now collected into the diagonal matrix ρ and the modal matrix Φ, respectively. The transformation

$$\begin{Bmatrix} u_I \\ q_1 \\ \hline q_2 \end{Bmatrix} = \begin{bmatrix} \Phi & 0 \\ 0 & I \end{bmatrix} \begin{Bmatrix} \xi \\ q_2 \end{Bmatrix} \tag{9}$$

Received Feb. 11, 1991; revision received May 27, 1991; accepted for publication June 6, 1991.

*Associate Professor, Department of Engineering Science and Mechanics. Associate Fellow AIAA.

is substituted into Eq. (7) to yield

$$\begin{bmatrix} I & m^T \\ m & I \end{bmatrix} \begin{Bmatrix} \ddot{\xi} \\ \ddot{q}_2 \end{Bmatrix} + \begin{bmatrix} \rho & 0 \\ 0 & \Lambda_2 \end{bmatrix} \begin{Bmatrix} \xi \\ q_2 \end{Bmatrix} = \begin{Bmatrix} 0 \\ 0 \end{Bmatrix} \tag{10}$$

where ξ represents an unknown modal displacement vector and

$$m = \begin{bmatrix} M_{IN2}^T & 0 \end{bmatrix} \Phi \tag{11}$$

Equation (10) represents the "exact" set of system equations in terms of the modal content ρ and Φ of the reduced model. Once a factor r^* is chosen and the eigenvalue problem (8) is solved, the user still has only marginal assurance that the solution converged to within the desired accuracy. Therefore, in practice, it is often necessary to solve another eigenvalue problem (10) where a limited number of frequencies in Λ_2 are retained. This procedure allows for some estimate of the convergence rate of the desired frequency range. It should be noted that this second eigenvalue problem can be solved more efficiently than the first one. Indeed, the user can assume that some degree of convergence is already achieved and can use the existing eigenvectors as starting vectors in some iterative method such as the subspace iteration method.

The objective in this paper, however, is to improve ρ and Φ at minimal cost based on realistically available information. First, it is assumed that at least some extra component modes are available, i.e., Λ_2 is not empty. Furthermore, it can only be assumed that those ϕ_i are available that correspond to $\rho_i < \Lambda_d$. If an improvement scheme is to make use of ϕ_i with frequencies higher than Λ_d, then the cost to compute these extra modes and frequencies must be included in the total cost of that scheme.

Many schemes are potentially suitable for improving the base solution ρ and Φ. However, these schemes are often costly, highly complicated, or make use of information not available in practice. Hasselman and Hart[10] developed a procedure based on the minimization of the Rayleigh quotient of the structure. Convergence of the individual frequencies and mode shapes can be achieved in only a few steps by employing the conjugate gradient technique in conjunction with an appropriate scaling transformation. The technique yields excellent results and is aimed at complete convergence of the base solution. In this paper, the aim is not complete convergence but consistent improvement at negligible cost. In addition, only practically available information is used, i.e., ϕ_i with corresponding frequencies $\rho_i < \Lambda_d$.

Convergence Improvement Scheme

The convergence scheme is designed to improve one eigenvalue-eigenvector pair ρ_i and ϕ_i at a time.

From Eq. (9), it follows that the base eigenvector corresponding to the base frequency ρ_i is given by

$$\begin{Bmatrix} u_I \\ q_1 \\ \hline q_2 \end{Bmatrix}_i = \begin{Bmatrix} \phi_i \\ 0 \end{Bmatrix} \tag{12}$$

where $\xi_i = e_i$ and $q_{2i} = 0$. The corrected eigenvector will be defined as

$$\begin{Bmatrix} u_I \\ q_1 \\ \hline q_2 \end{Bmatrix} = \begin{bmatrix} \Phi & 0 \\ 0 & I \end{bmatrix} \begin{Bmatrix} \xi_{0i} e_i \\ q_{2i} \end{Bmatrix} \tag{13}$$

$$\begin{Bmatrix} u_I \\ q_1 \\ \hline q_2 \end{Bmatrix} = \begin{Bmatrix} \xi_{0i} \phi_i \\ q_{2i} \end{Bmatrix} \tag{14}$$

in which $\lfloor \xi_{0i} \quad q_{2i}^T \rfloor^T$ is the eigenvector corresponding to the lowest eigenvalue λ_i of the following eigenvalue problem

$$\lambda \begin{bmatrix} 1 & m_i^T \\ m_i & I \end{bmatrix} \begin{Bmatrix} \xi_0 \\ q_2 \end{Bmatrix} = \begin{bmatrix} \rho_i & 0 \\ 0 & \Lambda_2 \end{bmatrix} \begin{Bmatrix} \xi_0 \\ q_2 \end{Bmatrix} \tag{15}$$

with

$$m_i = \begin{bmatrix} M_{IN2}^T & 0 \end{bmatrix} \phi_i \tag{16}$$

The corrected eigenvalue is defined as λ_i. Note that the improvement scheme for ρ_i and ϕ_i only requires the knowledge of ρ_i, ϕ_i, M_{IN2}, and λ_2. This information is minimal in the sense that it is absolutely needed if any correction is to be made at all.

Two important questions remain to be answered: 1) how to efficiently solve the eigenvalue problem in Eq. (15), and 2) does the solution computed from Eq. (15) indeed represent an improvement over the base solution ρ_i and ϕ_i? In the next section the first of these two questions will be answered.

Eigenvalue Problem

The eigenvalue problem (15) must be solved for the lowest eigenvalue and corresponding eigenvector. To this end, consider the lower partition of Eq. (15) and solve for q_2

$$q_2 = \lambda [\Lambda_2 - \lambda I]^{-1} m \xi_0 \tag{17}$$

where the subscript i has been deleted for convenience. The characteristic equation for this problem can then be obtained by substituting Eq. (17) into the top partition of Eq. (15)

$$\lambda - \rho + \lambda^2 m^T [\Lambda_2 - \lambda I]^{-1} m = 0 \tag{18}$$

This equation is easily solved for the lowest root via the Newton-Raphson iteration method

$$\lambda_{r+1} = \lambda_r - \frac{f(\lambda_r)}{f'(\lambda_r)} \tag{19}$$

in which r is the iteration index and

$$f(\lambda_r) = \lambda_r - \rho + \lambda_r^2 \sum_{j=1}^{N2} \frac{m_j^2}{\Lambda_{2j} - \lambda_r} \tag{20}$$

$$f'(\lambda_r) = 1 + 2\lambda_r \sum_{j=1}^{N2} \frac{m_j^2}{\Lambda_{2j} - \lambda_r} + \lambda_r^2 \sum_{j=1}^{N2} \frac{m_j^2}{(\Lambda_{2j} - \lambda_r)^2} \tag{21}$$

The iteration can be started with $\lambda_0 = \rho$. Because the Newton-Raphson method is quadratic and because only a good approximation of the lowest root is needed, no more than two iterations are recommended in Eq. (19). In addition, because the difference $\Lambda_{2j} - \lambda_r$ becomes larger with increasing j, all sums in Eqs. (20) and (21) can usually be truncated. This is particularly true for the third term in Eq. (21). In practice, therefore, the cost to obtain the lowest root of Eq. (18) is negligible.

The value of ξ_0 is obtained by requiring the corresponding eigenvector to be normal with respect to the mass matrix, i.e., the equation

$$\lfloor \xi_0 \quad q_2^T \rfloor \begin{bmatrix} 1 & m^T \\ m & I \end{bmatrix} \begin{Bmatrix} \xi_0 \\ q_2 \end{Bmatrix} = 1 \tag{22}$$

is solved for ξ_0 by substituing Eq. (17) into Eq. (22). It follows that

$$\xi_0 = \frac{1}{[f'(\lambda)]^{1/2}} \tag{23}$$

where λ is the converged lowest root of Eq. (18). Note that it can be proved that $f'(\lambda)$ is always positive.

In the next section, it will be shown that the newly computed eigenvalue-eigenvector pair does indeed constitute an improvement over the base solution.

Residual Vector Norm

Consider the eigenvalue problem $\lambda M\boldsymbol{u} = K\boldsymbol{u}$ corresponding to Eq. (1). Assuming the pair $\lambda, \boldsymbol{u}$ is an approximate solution, a residual vector $\boldsymbol{r}$ can be defined as

$$\boldsymbol{r} = (\lambda M - K)\boldsymbol{u} \tag{24}$$

The norm $|\boldsymbol{r}| = (\boldsymbol{r}^T\boldsymbol{r})^{1/2}$ of $\boldsymbol{r}$ is then an error measure for the pair λ, $\boldsymbol{u}$. Indeed, the smaller $|\boldsymbol{r}|$, the closer λ and $\boldsymbol{u}$ are to being an eigenvalue-eigenvector pair.

The residual vector $\boldsymbol{r}_i$ corresponding to the base solution can be obtained from Eqs. (7), (10), (12), and (24) as

$$\boldsymbol{r}_i = \begin{Bmatrix} 0 \\ \rho_i \boldsymbol{m}_i \end{Bmatrix} \tag{25}$$

and, therefore,

$$|\boldsymbol{r}_i| = \rho_i |\boldsymbol{m}_i| \tag{26}$$

The objective is to derive a similar residual vector norm for the improved solution and to compare it to the norm of Eq. (26). Using Eqs. (24), (10), and (14), the residual vector $\boldsymbol{r}_{ci}$ corresponding to the improved solution can be written as

$$\boldsymbol{r}_{ci} = \left(\lambda_i \begin{bmatrix} I & m^T \\ m & I \end{bmatrix} - \begin{bmatrix} \rho & 0 \\ 0 & \Lambda_2 \end{bmatrix}\right)\begin{Bmatrix} \xi_{0i}\boldsymbol{e}_i \\ \boldsymbol{q}_{2i} \end{Bmatrix}$$

$$= \begin{Bmatrix} (\lambda_i I - \rho)\xi_{0i}\boldsymbol{e}_i + \lambda_i m^T \boldsymbol{q}_{2i} \\ \lambda_i m\, \xi_{0i}\boldsymbol{e}_i + (\lambda_i I - \Lambda_2)\boldsymbol{q}_{2i} \end{Bmatrix} \tag{27}$$

The bottom partition of Eq. (27) vanishes because of the bottom partition of Eq. (15). In addition, row i of the top partition of Eq. (27) also vanishes because of the top partition of Eq. (15). Therefore, Eq. (27) reduces to

$$\boldsymbol{r}_{ci} = \begin{pmatrix} \lambda_i \boldsymbol{m}_i^T \boldsymbol{q}_{2i} \\ 0 \end{pmatrix} \tag{28}$$

where $\boldsymbol{m}_i$ is identical to $\boldsymbol{m}$ except that the ith column is replaced by 0. Therefore, the exact norm is

$$|\boldsymbol{r}_{ci}| = \lambda_i |\boldsymbol{m}_i^T \boldsymbol{q}_{2i}| \tag{29}$$

It will now be shown that under certain conditions this norm is always smaller than the norm in Eq. (26). Note that in the context of norm calculations, the matrix $\boldsymbol{m}_i$ can now be considered as the matrix $\boldsymbol{m}$ from which the ith column is removed. Following the rules for norm manipulation, it follows from Eq. (29) that

$$|\boldsymbol{r}_{ci}| \le \lambda_i |\boldsymbol{m}_i^T|\, |\boldsymbol{q}_{2i}| \tag{30}$$

In order to estimate $|\boldsymbol{m}_i^T|$, consider the following matrix

$$\begin{bmatrix} I & \boldsymbol{m}_i^T \\ \boldsymbol{m}_i & I \end{bmatrix} = \begin{bmatrix} I & 0 \\ 0 & I \end{bmatrix} + \begin{bmatrix} 0 & \boldsymbol{m}_i^T \\ \boldsymbol{m}_i & 0 \end{bmatrix}$$

$$\stackrel{\text{def}}{=} I + M_i \tag{31}$$

This matrix is obtained from the mass matrix in Eq. (10) by omitting the ith row and column. Therefore, it represents the mass matrix for a system with constraint $\xi_i = 0$. It follows then that the matrix on the left side of Eq. (31) is still positive definite. Consequently, because $\boldsymbol{x}^T\boldsymbol{x}$ is positive (for all $\boldsymbol{x}$ nonzero), it can be seen that

$$1 + \frac{\boldsymbol{x}^T M_i \boldsymbol{x}}{\boldsymbol{x}^T\boldsymbol{x}} > 0 \tag{32}$$

The second term on the left side of inequality (32) is the Rayleigh quotient, say R_i for the matrix M_i so that

$$R_i > -1 \tag{33}$$

Furthermore, R_i has the property

$$\mu_{li} \le R_i \le \mu_{hi} \tag{34}$$

in which μ_{li} and μ_{hi} are the lowest and highest eigenvalues of M_i, respectively. R_i can in fact reach μ_{li} only when $\boldsymbol{x}$ is the corresponding eigenvector. Hence, Eqs. (33) and (34) yield

$$-1 < \mu_{li} \tag{35}$$

Next, consider the eigenvalue problem for M_i

$$\begin{bmatrix} 0 & \boldsymbol{m}_i^T \\ \boldsymbol{m}_i & 0 \end{bmatrix}\begin{Bmatrix} y_1 \\ y_2 \end{Bmatrix} = \mu \begin{Bmatrix} y_1 \\ y_2 \end{Bmatrix} \tag{36}$$

From the structure of this eigenvalue problem, it follows that the eigenvalues of M_i are symmetric with respect to zero. This fact, together with inequality (35) leads to the conclusion that all eigenvalues μ_i of M_i satisfy

$$-1 < \mu_i < 1 \tag{37}$$

Next, by definition,[11]

$$|\boldsymbol{m}_i^T| = \max_{y \ne 0} \frac{|\boldsymbol{m}_i^T \boldsymbol{y}|}{|\boldsymbol{y}|} \tag{38}$$

This equation can be rewritten as follows:

$$|\boldsymbol{m}_i^T|^2 = \max_{y \ne 0} \frac{\boldsymbol{y}^T(\boldsymbol{m}_i \boldsymbol{m}_i^T)\boldsymbol{y}}{\boldsymbol{y}^T\boldsymbol{y}} \tag{39}$$

The right-hand side of Eq. (39) is equivalent to the maximum of the Rayleigh quotient corresponding to the matrix $\boldsymbol{m}_i\boldsymbol{m}_i^T$. Because of the conclusions drawn from Eq. (36), it can now be stated that

$$|\boldsymbol{m}_i^T| = |\mu_{li}| = \mu_{hi} < 1 \tag{40}$$

Combining Eqs. (30) and (40) leads to

$$|\boldsymbol{r}_{ci}| < \lambda_i \mu_{hi} |\boldsymbol{q}_{2i}| \tag{41}$$

Furthermore, from Eqs. (41) and (17) and the fact that $|(\Lambda_2 - \lambda_i I)^{-1}| = 1/(\Lambda_{21} - \lambda_i)$, it follows that

$$|\boldsymbol{r}_{ci}| < \frac{\xi_{0i}\mu_{hi}\lambda_i^2}{\Lambda_{21} - \lambda_i} |\boldsymbol{m}_i| \tag{42}$$

where Λ_{21} is the smallest value on the diagonal of Λ_2. The right-hand side of inequality (42) is another computable upper bound, directly comparable to the norm $|\boldsymbol{r}_i|$ of the base solution, as given by Eq. (26).

In order for the suggested improved solution to actually be better than the base solution, it is necessary that

$$\frac{\xi_{0i}\mu_{hi}\lambda_i^2}{\Lambda_{21} - \lambda_i} < \rho_i \tag{43}$$

This follows from comparing Eq. (26) with inequality (42). Inequality (43) implies the knowledge of μ_{hi}, which would

require the solution of the eigenvalue problem (36) for its highest (or lowest) eigenvalue. To avoid this cost, inequality (43) can be made somewhat more stringent by invoking Eq. (40) and demanding that

$$\frac{\xi_{0i}\lambda_i^2}{\Lambda_{21}-\lambda_i} < \rho_i \tag{44}$$

It can then be stated that, if inequality (44) is fulfilled, a better solution than the base solution is obtained. If not, the base solution should be retained.

In addition, an a priori condition for consistent improvement can be derived by noting that

$$\xi_{0i} \le 1, \qquad \lambda_i \le \rho_i \qquad \text{all } i \tag{45}$$

and by requiring that

$$\frac{\rho_i}{\Lambda_{21}-\rho_i} < 1 \qquad \text{or} \qquad \Lambda_{21} > 2\rho_i \tag{46}$$

Inequality (46) would therefore require the user to employ a factor r^* of at least 2 in Eq. (5). Fortunately, this is the minimum value for r^* used in practice. In fact, inequality (46) may very well be the reason why the empirical minimum value for r^* is 2. Consequently, if standard truncation practices are followed, the convergence improvement scheme will always result in better eigenvalue-eigenvector pairs.

Finally, from Eqs. (26), (40), (42), and (45), it follows that

$$|r_{ci}| \le \frac{\rho_i}{\Lambda_{21}-\rho_i}|r_i| \tag{47}$$

It should be noted that criterion (46) is sufficient but not necessary. This means that results are often better than inequality (47) would suggest. Relationship (47) provides an indicator as to how the improvement depends on ρ_i.

Implementation

In order to improve a typical eigenvalue-eigenvector pair ρ_i and ϕ_i, the following steps must be taken.

Step 1

Compute m_i from Eq. (16) repeated here as Eq. (48)

$$m_i = \begin{bmatrix} M_{IN2}^T & 0 \end{bmatrix} \phi_i \tag{48}$$

This step requires $N_2 \times I$ flops (floating point operations), where N_2 is the number of added component modes and I is the number of interface degrees of freedom.

Step 2

Solve the eigenvalue problem (15) for the lowest eigenvalue and corresponding eigenvector (subscript i is omitted)

For $j = 1,\ldots,N_2$

$s_j := m_j^2$ (save)

$\lambda_0 := \rho$

For $r = 0,1,\ldots$

$S_1 := 0,\ S_2 := 0$

For $k = 1,2,\ldots,N_2$

$a := \Lambda_{2k} - \lambda_r$

b $:= s_k$

$S_1 := S_1 + b$

$S_2 := S_2 + b/a$

$$f(\lambda_r) := \lambda_r - \rho + \lambda_r^2 S_1$$

$$f'(\lambda_r) := 1 + 2\lambda_r S_1 + \lambda_r^2 S_2$$

$$\lambda_r := \lambda_r - f(\lambda_r)/f'(\lambda_r) \tag{49}$$

Ordinarily, no more than two iterations are necessary to obtain an adequate solution. In addition, the summations S_1 and S_2 can often be truncated because $a := \Lambda_{2k} - \lambda_r$ becomes increasingly larger with increasing k. Without these cost reductions, this algorithm requires on the order of $2rN_2$ flops where r is the number of iterations.

Step 3

Compute ξ_0 from Eq. (23) repeated here as Eq. (50)

$$\xi_0 = \frac{1}{[f'(\lambda)]^{1/2}} \tag{50}$$

where λ_r is the converged frequency obtained from Eq. (49)

Step 4

The updated eigenvector is computed from Eqs. (14) and (17) where subscript i is again omitted for simplicity

For $k = 1,2,\ldots,N_2$

$q_{2k} := \lambda_r m_k \xi_0/(\Lambda_{2k})$

For $j = 1,2,\ldots,I+N_1$

$u_j := \xi_0 \phi_j$ (51)

where u represents the first partition in Eq. (14). This computation requires approximately $2N_2 + I + N_1$ flops.

Therefore, updating a typical eigenvalue-eigenvector pair ρ_i, ϕ_i requires at most $(I + 2r + 2)N_2 + I + N_1$ flops. In practice, this cost is negligible compared to the cost of obtaining the base solution in the first place. In the next section, several demonstration problems will be considered.

Demonstration Problems

As a first example, consider the planar truss in Fig. 1. This truss consists of 20 bays. The first 12 bays are taken as component A and the remaining 8 as component B. Each of the bays consists of individual two-dimensional truss members made of an aluminum alloy with Young's modulus $E = 71.02$ GPa and mass density $\rho^* = 2685$ kg/m^3. The horizontal and vertical members are $L = 1$ m long and have circular cross sections of diameter $d = 0.01$ m. Each node in this structure has two displacement degrees of freedom, i.e., the x and y

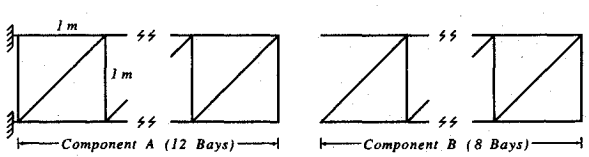

Fig. 1 Twenty bay planar truss.

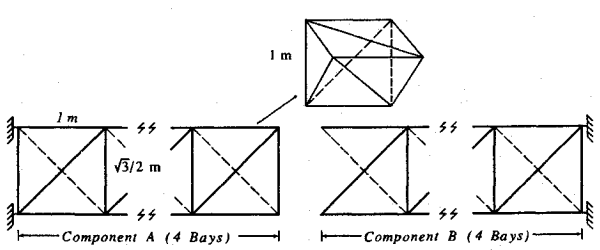

Fig. 2 Eight bay spatial truss.

displacements u and v. The structure is restrained at the left end, and therefore, component A has 48 degrees of freedom, component B has 36, and the overall structure has 80. The interface between components A and B contains four degrees of freedom.

The first step in the analysis is to apply, for example, the Craig/Bampton procedure to components A and B and explicitly produce Eq. (10). The eigenvalue problem corresponding to Eq. (10) is then solved and considered as the "exact" solution. The first seven frequencies in Hz units are listed in the first column of Table 1 under the heading "Exact f, Hz". Next, two cases are considered. In the first case, it is desired that $f_d = (\Lambda_d^{1/2})/2\pi$ is 50 Hz and in the second case it is desired that $f_d = 100$ Hz. In both cases, the factor r^* in Eq. (5) is taken as 2. Recall that $r^* = 2$ represents the minimum value of r^* for which the presented convergence improvement scheme yields unconditional improvement for all frequencies less than f_d. Recall that at the Hertz level the factor 2 becomes $\sqrt{2}$, i.e., for case 1 $f_c = \sqrt{2}\,50$ Hz ≈ 71 Hz, and furthermore, for case 2, $f_c = \sqrt{2}\,100$ Hz ≈ 142 Hz.

For explanatory purposes, consider the five subcolumns in Table 1 under the heading "Case 1, $f_d = 50$ Hz." The first subcolumn f_b displays the base frequencies, i.e., the frequencies in Hz corresponding to the eigenvalue problem in Eq. (8). In a standard component mode synthesis solution, these frequencies would represent the final result and all mode shapes with frequencies less than 50 Hz would be retained for subsequent response calculations. The second subcolumn e_b lists the percentage relative error between f and f_b

$$e_b = \frac{f_b - f}{f} \times 100 \tag{52}$$

The third subcolumn f_i contains the improved frequencies based on the presented improvement scheme. Then, the fourth subcolumn e_i displays the percentage relative error between f and f_i

$$e_i = \frac{f_i - f}{f} \times 100 \tag{53}$$

Finally, the fifth subcolumn e lists

$$e = \left(1 - \frac{|e_i|}{|e_b|}\right) \times 100 \tag{54}$$

Table 1 Results for planar truss

N	Exact f, Hz	Case 1, $f_d = 50$ Hz[a]					Case 2, $f_d = 100$ Hz[b]				
		f_b	e_b	f_i	e_i	e	f_b	e_b	f_i	e_i	e
1	2.3664	2.3665	0.002	2.3664	7.e-9	100	2.3664	5.e-4	2.3664	1.e-10	100
2	13.852	13.878	0.2	13.852	−2.e-4	100	13.855	2.e-2	13.852	−5.e-6	100
3	35.459	35.662	0.6	35.458	−4.e-3	99	35.519	0.17	35.459	−4.e-4	100
4	43.379	45.814	6.0	43.364	−4.e-2	99	43.702	0.75	43.379	2.e-4	100
5	63.072	74.459	18.0	61.807	−2.e-0	89	63.120	8.e-2	63.071	−7.e-4	99
6	93.817						96.739	3.0	93.757	−6.e-2	98
7	126.74						137.88	9.0	122.30	−3.e-0	60

[a] Frequencies above dashed line are less than 50 Hz.
[b] Frequencies above dashed line are less than 100 Hz.

Table 2 Results for spatial truss (eight bays)

N	Exact f, Hz	Case 1, $f_d = 50$ Hz[a]					Case 2, $f_d = 100$ Hz[b]				
		f_b	e_b	f_i	e_i	e	f_b	e_b	f_i	e_i	e
1	46.075	48.228	4.7	46.075	1.e-4	100	46.188	0.25	46.075	1.e-4	100
2	46.075	48.228	4.7	46.075	1.e-4	100	46.188	0.25	46.075	1.e-4	100
3	49.906	54.121	8.4	49.906	4.e-5	100	50.055	0.30	49.906	4.e-4	100
4	98.962	186.75	88.7	500.14	405.0	−360	98.972	0.01	98.962	4.e-5	100
5	103.86						103.90	0.04	103.86	1.e-4	100
6	103.86						103.90	0.04	103.86	1.e-4	100
7	146.14						158.92	8.7	145.17	−0.7	92
8	172.63						186.30	7.9	171.44	−0.7	91

[a] Frequencies above dashed line are less than 50 Hz.
[b] Frequencies above dashed line are less than 100 Hz.

Table 3 Results for spatial truss (32 bays)

N	Exact f, Hz	Case 1, $f_d = 15$ Hz[a]					Case 2, $f_d = 25$ Hz[b]				
		f_b	e_b	f_i	e_i	e	f_b	e_b	f_i	e_i	e
1	3.8413	3.8461	0.1	3.8413	1.e-5	100	3.8461	0.1	3.8413	1.e-5	100
2	3.8413	3.8461	0.1	3.8413	1.e-5	100	3.8461	0.1	3.8413	1.e-5	100
3	10.263	10.277	0.1	10.263	4.e-4	100	10.277	0.1	10.263	4.e-4	100
4	10.263	10.277	0.1	10.263	4.e-4	100	10.277	0.1	10.263	4.e-4	100
5	12.275	13.490	10	12.275	6.e-6	100	12.328	0.4	12.275	1.e-3	100
6	19.375	20.188	4	19.314	−0.3	92	20.188	4	19.314	−0.3	92
7	19.375	20.188	4	19.314	−0.3	92	20.188	4	19.314	−0.3	92
8	24.538	52.160	112.	58.358	138.	−224	24.539	0.001	24.538	1.e-6	100
9	30.692						42.411	38	36.302	18	52

[a] Frequencies above dashed line are less than 50 Hz.
[b] Frequencies above dashed line are less than 25 Hz.

where e represents the percentage of the total error e_b, which was captured by the improvement scheme.

As expected, all frequencies less than 50 Hz (those above the dashed line in Table 1) experience a significant improvement; in fact, the improvement scheme captures more than 99% of the error in all frequencies. It turns out that even some of the frequencies above 50 Hz benefit from the scheme, although this cannot be guaranteed and should not be trusted. It should also be noted that the improved frequencies could be either below or above the exact frequency. This is due to the fact that the correction procedure only involves the mass and stiffness matrix rows and columns corresponding to the frequency that is being corrected. Consequently, leaving out the remaining rows and columns may result in an estimate that is either higher or lower than the exact frequency. However, in either case, the eigenvalue-eigenvector pair will be better than the base pair. Finally, it is also worth noting that the scheme in Eq. (49), on the average, only required two iterations per frequency in order to converge to within 0.001 percentage relative error.

A second example is presented in Fig. 2. A three-dimensional truss is considered that consists of two four-bay components A and B. The overall structure is restrained at both ends. Both components then have 36 degrees of freedom and the overall structure has 63. The individual truss members have the same E, ρ^*, and d as in the first example, and the dimensions of a typical bay are shown in Fig. 2.

Two different desired fidelities are investigated, $f_d = 50$ and 100 Hz. The corresponding results are displayed in Table 2. For case 1, it should be noted that even the first two base frequencies are off by 4.7%. All frequencies lower than 50 Hz (above the dashed line in Table 2) are fully corrected, and those larger than 50 Hz may or may not improve. This is again consistent with the theory. For case 2, it can be seen that the base solution is in fact more than adequate and no correction is needed. However, this is not known in advance and, in order to verify that the base solution has indeed converged, the analyst would need to solve an additional eigenvalue problem with $f_d > 100$ Hz. Note that, for frequencies less than 100 Hz, the improved frequencies are almost identical to the exact frequencies.

The third and final example is identical to the second, except that both structural components now consist of 16 bays. Components A and B, therefore, have 144 degrees of freedom, and the overall structure has 279. Table 3 lists the results for case 1, $f_d = 15$ Hz and case 2, $f_d = 25$ Hz.

Conclusions

A method is derived to consistently improve the base system frequencies and mode shapes obtained via standard component mode synthesis techniques. The method is aimed at reducing the value of the residual norm associated with each of the base eigenvalue-eigenvector pairs. Although the proposed scheme does not yield complete convergence, significant improvement is consistently realized at very little cost, requiring only reading available information. In addition, the technique gives the analyst a good idea of the degree of convergence achieved in the base eigenvalue-eigenvector pairs without having to solve an extra system eigenvalue problem.

The implementation of the scheme can be accomplished in the form of a postprocessor, so that component mode synthesis computer programs need not be altered. Finally, it should also be noted that the demonstration problems as well as additional experience show that, if the convergence improvement scheme is used, the cutoff frequency need not be taken larger than twice the desired system fidelity in order to achieve acceptable convergence.

References

[1]Hurty, W. C., "Dynamic Analysis of Structural Systems Using Component Modes," *AIAA Journal,* Vol. 3, No. 4, 1965, pp. 678–685.

[2]Craig, R. R., and Bampton, M. C. C., "Coupling of Substructures for Dynamic Analysis," *AIAA Journal,* Vol. 6, No. 7, 1968, pp. 1313–1319.

[3]MacNeal, R. H., "A Hybrid Method of Component Mode Synthesis," *Computers & Structures,* Vol. 1, Dec. 1971, pp. 581–601.

[4]Benfield, W. A., and Hruda, R. F., "Vibration Analysis of Structures by Component Mode Substitution," *AIAA Journal,* Vol. 9, No. 7, 1971, pp. 1255–1261.

[5]Rubin, S., "Improved Component-Mode Representation for Structural Dynamic Analysis," *AIAA Journal,* Vol. 13, No. 8, 1975, pp. 995–1006.

[6]Hou, S., "Review of Modal Analysis Techniques and a New Approach," *Shock and Vibration Bulletin,* No. 40, Pt. 4, Dec. 1969, pp. 25–39.

[7]Craig, R. R., "Methods of Component Mode Synthesis," *Shock and Vibration Digest,* Vol. 9, Nov. 1977, pp. 3–10.

[8]Engels, R. C., Craig, R. R., and Harcrow, H. W., "A Survey of Payload Integration Methods," *Journal of Spacecraft and Rockets,* Vol. 21, No. 5, 1984, pp. 417–424.

[9]Engels, R. C., "Dynamic Finite Element Modeling of Some Basic Structural Members," *Proceedings of the 1990 ASME International Computers in Engineering Conference,* edited by G. L. Kinzel and S. M. Rohde, Vol. 1, American Society of Mechanical Engineers, New York, 1990, pp. 493–503; also *Journal of Vibration and Acoustics* (to be published).

[10]Hasselman, T. K., and Hart, G. C., "A Minimization Method for Treating Convergence in Modal Synthesis," *AIAA Journal,* Vol. 12, No. 3, 1974, pp. 316–322.

[11]Golub, G. H., and Van Loan, C. F., *Matrix Computations,* Johns Hopkins University Press, Baltimore, MD, 1985.